Electric-stress reliability and current collapse of different thickness SiN_x passivated AlGaN/GaN high electron mobility transistors*

Yang Ling(杨 凌)†, Hu Gui-Zhou(胡贵州), Hao Yue(郝 跃)‡, Ma Xiao-Hua(马晓华), Quan Si(全 思), Yang Li-Yuan(杨丽媛), and Jiang Shou-Gao(姜守高)

Key Laboratory for Wide Band-Gap Semiconductor Materials and Devices, School of Microelectronics, Xidian University, Xi'an 710071, *China*

(Received 16 June 2009; revised manuscript received 4 August 2009)

This paper investigates the impact of electrical degradation and current collapse on different thickness SiN_x passivated AlGaN/GaN high electron mobility transistors. It finds that higher thickness SiN_x passivation can significantly improve the high-electric-field reliability of a device. The degradation mechanism of the SiN_x passivation layer under ON-state stress has also been discussed in detail. Under the ON-state stress, the strong electric-field led to degradation of SiN_x passivation located in the gate-drain region. As the thickness of SiN_x passivation increases, the density of the surface state will be increased to some extent. Meanwhile, it is found that the high NH_3 flow in the plasma enhanced chemical vapour deposition process could reduce the surface state and suppress the current collapse.

Keywords: SiN_x passivated AlGaN/GaN high electron mobility transistors, degradation, current collapse, surface states

PACC: 7320, 7280E, 7360L

1. Introduction

GaN high electron mobility transistors (HEMT) have demonstrated outstanding performance in radio frequency (RF) power and high voltage switching applications.[1,2] Although the reliability of GaN HEMTs has been improving,[3] these devices still suffer from a variety of degradation mechanisms.[4−9] One of the most deleterious effects of electrical degradation is an increase in carrier trapping and subsequent current collapse.[4,6−11] Consequently, charge carrier can reach very high energies, and trigger hot-carrier degradation phenomena, such as charge trapping, defects, and/or deep-level trap generation. Moreover, high drain-source voltage V_{DS} values may lead to RF power dissipation and thermal mismatch or strain due to piezoelectric effects.[12] As is well known, the effect that most severely limits the RF power performance of AlGaN/GaN HEMTs is the so-called RF current collapse or RF power slump, which originates from trapping effects at the device surface and/or in the buffer.[13] It has been suggested that these traps act as a "surface-charge-control" layer, which reduces the effect of surface polarization charge.[14] Although the SiN_x passivation layer can improve the high-electric-field reliability and current collapse, few physicists have studied the relationship among the SiN_x growth conditions, the reliability and the current collapse of devices.

In this work, we have investigated the impact of electrical degradation and current collapse on passivated AlGaN/GaN HEMT with different SiN_x thickness and recipes in the plasma enhanced chemical vapour deposition (PECVD) process, with the following specific aims: 1) analysis of the degradation mechanism of the SiN_x passivation layer under ON-state stress, 2) thick SiN_x passivation can significantly improve the high-electric-field reliability of device, 3) as the NH_3 flow in PECVD process increases, the density of the surface state will decrease.

2. Device and experiments

The $Al_xGa_{1-x}N$/GaN HEMT shown in this work was grown on (0001) sapphire substrate using metalor-

*Project supported by the State Key Program of National Natural Science Foundation of China (Grant No. 60736033).

†Corresponding author. E-mail: yangling_60@yahoo.cn

‡E-mail: yhao@xidian.edu.cn

© 2010 Chinese Physical Society and IOP Publishing Ltd

ganic chemical vapour deposition. The HEMT heterostructure comprised a semi-insulating GaN buffer and an AlGaN barrier. Cl_2/BCl_3 plasma was used for the mesa isolation. The Ohmic contacts were obtained by deposition of a Ti/Al/Ni/Au multilayer, followed by rapid-thermal annealing at 850 °C for 30 s in an N_2 ambience. Devices were fabricated using L-shape gate technology with a centred 0.4-μm gate length and 0.7 μm field plate. The drain-source spacing was 3 μm.

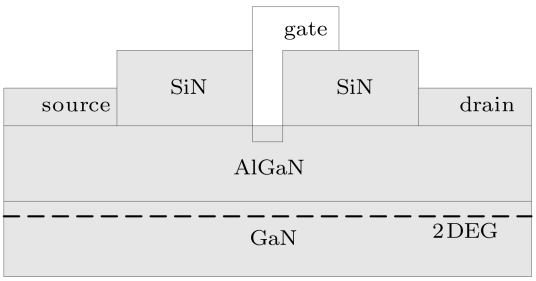


Fig. 1. Schematic diagram of the AlGaN/GaN HEMT structure.

The 40-nm and 80-nm thickness SiN_x passivation was deposited by silane/NH_3-based PECVD. The SiN_x film was etched by CF_4/O_2 plasma at room temperature. Two different recipes were employed: (i) 2-sccm NH_3 flow SiN_x deposited at 250 °C (device A and device B), (ii) 2.5-sccm NH_3 flow SiN_x also deposited at 250 °C (device C). For comparison, three different kinds of AlGaN/GaN HEMTs were fabricated on sapphire substrates—40-nm (device A) and 80-nm (device B and device C) SiN_x passivation. Figure 1 shows a schematic diagram of the device structure.

3. Results and discussion

The SiN_x passivated HEMT was stressed under the ON-state situation. Direct current (DC) characteristics were measured at several time intervals after the stress started. Pulse I–V characteristics have been measured by using gate and drain pulsing, and the quiescent bias point was ($V_G = 0$ V, $V_{DS} = 15$ V). The pulse duration was 500 ns with a 1-ms period. Twenty minute intervals between the measurements avoided memory effects related to trapping. A high-electric-field stress campaign was carried out on the devices in order to evaluate their stability. Under the ON-state electric-stress conditions, both thermally induced and hot-electron-related degradation can occur. For ON-state stress, V_{DS} and V_{GS} were set to 20 V and 0 V respectively. All the tested devices exhibited the degradation effects described in the following.

The SiN_x passivation layer with different thickness played a different role in the surface state density and concentration of the two-dimensional electron gas (2DEG), leading to differences in both I_{DS} and G_m for devices A and B. As can be noted in Figs. 2(a) and 3(a), the I_{DS} drop induced by the stress is maximum at high V_{GS} and V_{DS} (i.e., under the saturation region) and low V_{DS} (i.e., in the linear region of the I–V curves). This kind of behaviour is generally attributed to the increase in the drain access resistance R_D, resulting from electron trapping in the SiN_x passivation or in the gate-drain channel access region, at the device surface and/or in the layers underneath the channel.[15] The degradation of device A in the linear region was significant (Fig. 2(a)), while device B was almost unchanged in this region. A similar situation happened in the saturation region (Fig. 3(a)).

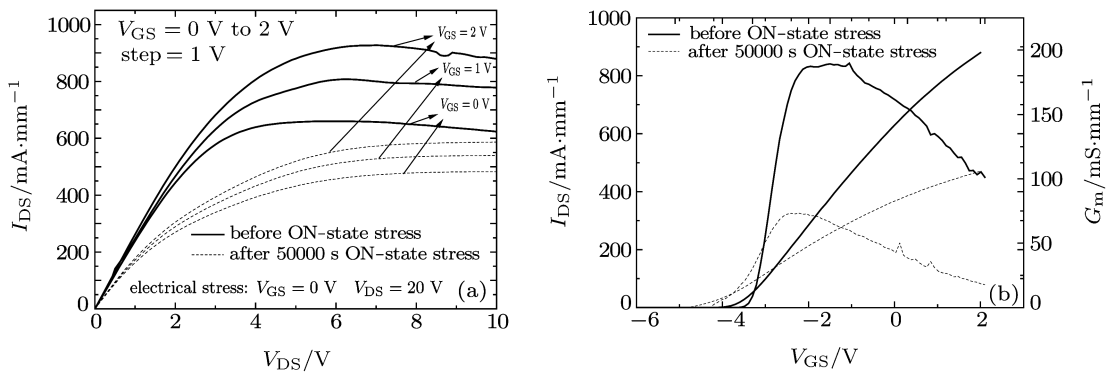


Fig. 2. Source-drain output curves and transfer curves of the 40-nm thickness SiN_x passivated AlGaN/GaN HEMTs (device A) before and after 50000 s ON-state stress.

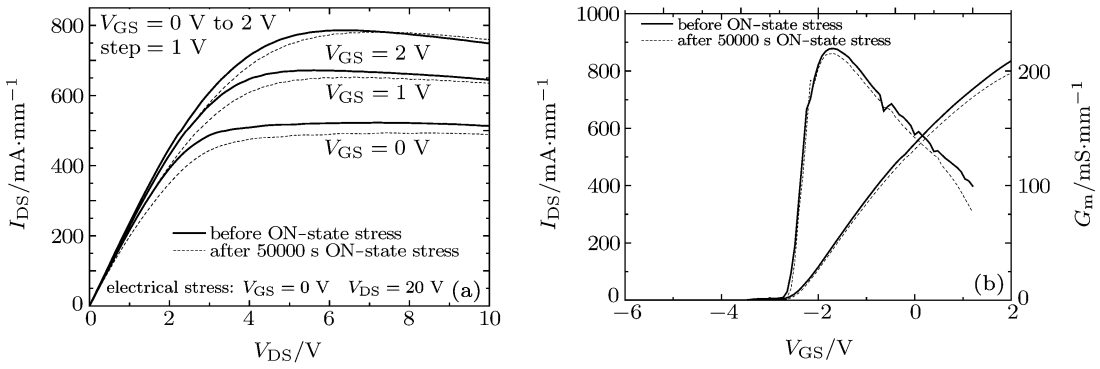


Fig. 3. Source-drain output curves and transfer curves of the 80-nm thickness SiN_x passivated AlGaN/GaN HEMTs (device B) before and after 50000 s ON-state stress.

The devices A and B have the same epitaxial structure and process, and the main difference is the passivation layer thickness. Then, the reasons for the degradation of I_{DS} were interface charge between the SiN_x and AlGaN, and the electron traps in the SiN_x passivation.

A drastic decrease in I_{max}, and G_{max} were observed in device A as a result of stress, in contrast, the electrical properties of device B had a very small degradation (Fig. 4(a)). Figure 4(b) shows I_G versus V_{DS} curves measured before and after the ON-state stress (50000 s). Two phenomena can contribute to this I_G drop, namely 1) a decrease in the surface conductance between gate and drain and 2) a reduction of the gate-drain electric field lowering the electron injection from the gate. Both 1) and 2) are consistent with the hypothesis of damaged gate-drain surface invoked to explain all other degradation modes. The first effect actually derived from the generation of deeper acceptor-like traps, compensating the preexisting relatively shallow donor and, thus, lowering the surface free electron density between the gate and drain contacts. The second one can be induced by reduced positive ionized charge. That can increase the gate barrier thickness, resulting in gate-leakage reduction. The latter mechanism is, in many respects, similar to the so-called "breakdown walkout", a well-known effect of hot-electron stress observed in GaAs-based field effect transistors and attributed to the increase in the surface-trap density.[16] The same effects could also be induced by electron trapping and accumulation into preexisting deep levels at the device surface. Figure 4(b) indicated that the device B surface had more electron traps than that of device A. Therefore, the surface electron filling effect of device B was more obvious than that of device A.

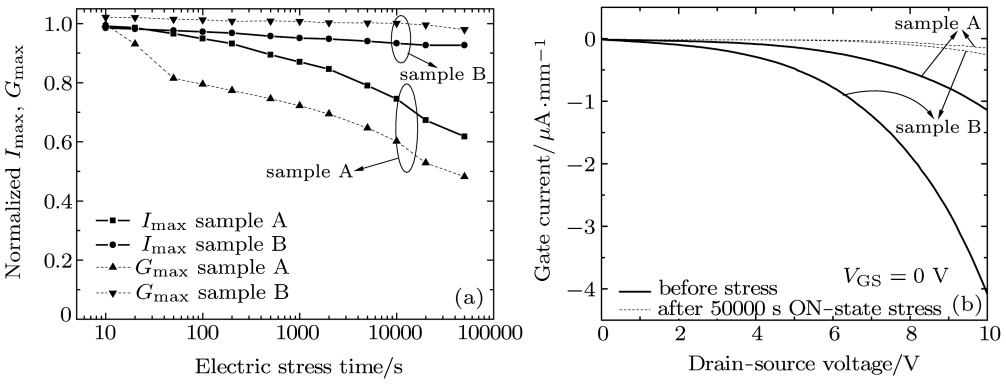


Fig. 4. (a) The DC characteristics (I_{max}, G_m) as a function of high electric-field stress time, (b) static I_G versus V_{DS} characteristics measured before (solid) and after (dashed) 50000 s of ON-state stress.

The capacitance and conductance measurements in the frequency were used to characterize the trapping effects in the prepared device A and device B. Assuming a continuum of trap levels, we can express the equivalent parallel capacitance C_p and conductance G_p as functions of frequency, as[17]

$$C_p = C_b + \frac{qD_T}{\omega\tau_T \tan(\omega\tau_T)},$$

and

$$\frac{G_{\rm p}}{\omega} = \frac{qD_{\rm T}}{2\omega\tau_{\rm T}} \ln(1 + (\omega\tau_{\rm T})^2),$$

where $D_{\rm T}$ is the trap density, $\tau_{\rm T}$ is the trap state time constant, $C_{\rm b}$ is the barrier capacitance, and ω is the radial frequency. The $D_{\rm T}$ and $\tau_{\rm T}$ quantities can be extracted by fitting the experimental $C_{\rm p}(\omega)$ or $G_{\rm p}(\omega)$ data. Typical $G_{\rm p}/\omega$ versus ω curves for the AlGaN/GaN, measured at selected biases near the threshold voltage, are shown in Fig. 5(a). From the fitting resulting parameters of device A, $D_{\rm T(f)} = 2.38 \times 10^{12}$ cm^{-2}·eV^{-1}. On the other hand, fitting of $G_{\rm p}/\omega$ data for device B yielded $D_{\rm T(f)} = 1.17 \times 10^{13}$ cm^{-2}·eV^{-1}. The density of the electron traps in device B is nearly one order of magnitude higher than that in device A. The electron trap density contributed to the surface states. In Fig. 5(b), although device B had a thicker SiN_x passivation layer, the current collapse of device B is more serious than that of device A, about 29% and 56% of drain current collapse for devices A and B, respectively. This showed that the thick passivation layer will increase the surface density of states which was caused by tensive and compressive stress between the SiN_x and AlGaN, exacerbating the current collapse. The content of Fig. 5(b) further confirmed the results of Fig. 5(a).

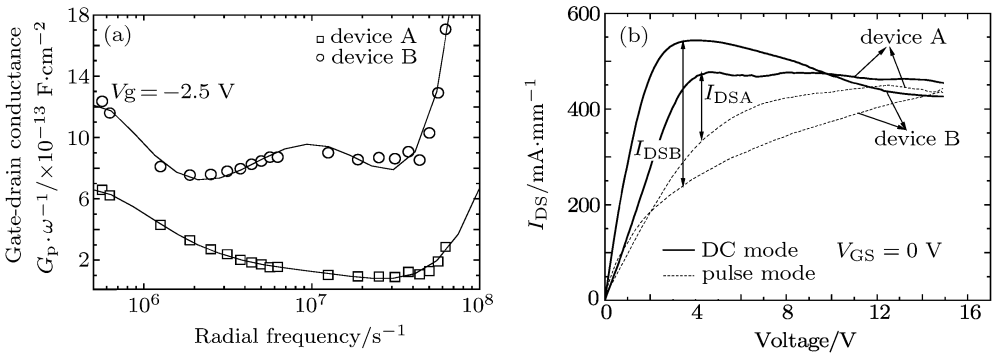


Fig. 5. (a) Gate-drain conductance as a function of frequency for AlGaN HEMTs (full lines are fitting curves). (b) Experimental $I_{\rm D}$–$V_{\rm DS}$ characteristics obtained in DC and in the gate turn-on mode. The pulse width is 500 ns with a 1-ms period.

Figure 6 schematically indicates how the surface state charge causes the current collapse. This surface state charge trapped the electrons changing into the negative charge, and the surface potential is made negative, depleting the channel of electrons and leading to extension of the gate depletion region. Therefore, the source-drain current is controlled by the gate voltage and the total amount of trapped charge in the gate drain access region. As a result of the high surface state density in device B, there are more electrons filling into the surface states. Therefore, the current collapse of device B is more serious than that of device A.

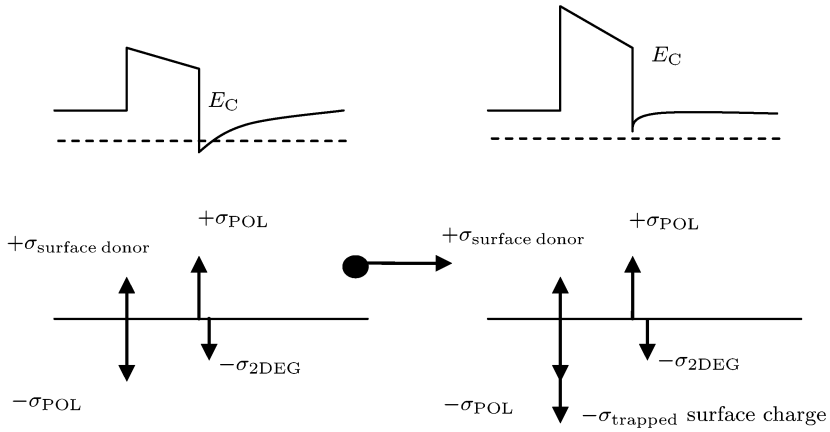


Fig. 6. Band diagram of the AlGaN/GaN heterostructure showing that the surface trapped charge reduces the effective donor density and thus leads to a current collapse.

Why did device B with a larger density of surface state have less degradation after 50000 s ON-state stress? This is because the electrical property degradation of devices relates not only to the surface states, but also to the electron trap formation in SiN_x passivation between the gate and drain access region under the condition of ON-state stress. As a result of the thin SiN_x passivation of device A, the internal electric field of SiN_x passivation was larger and it was prone to generating electron traps. In Fig. 7, the leakage of SiN_x passivation for device A occurred in a significant increase under electric field. This indicated that the thin SiN_x passivation easily formed the conductive channels—electron traps.

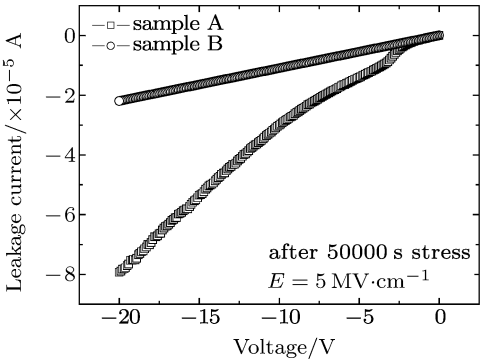


Fig. 7. Leakage characteristics for SiN_x passivation with different thickness.

We simulated the electric field profiles in SiN_x passivation along the 2DEG channel direction. The results show that the peak electric field in thin SiN_x passivation is much larger than that of the thick one in Fig. 8. The larger peak electric field inevitably leads to degradation of SiN_x passivation, and the electron traps simultaneously form. Therefore, the degradation of SiN_x passivation between gate and drain is the main reason for the device degradation under the ON-state stress.

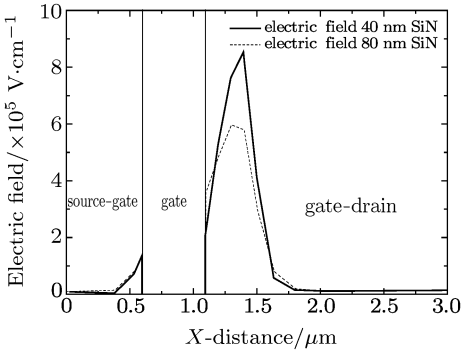


Fig. 8. The simulated electric field profiles in SiN_x passivation between source and drain.

With an increase of NH_3 flow in the PECVD process, device C kept a good electrical reliability (in Fig. 9(a)). At the same time, the drain current collapse is reduced from 56% (device B) to 41% (device C) in Fig. 9(b). From the fitting resulting parameters of device C, the trap density is reduced from 1.17×10^{13} cm^{-2}·eV^{-1} (device B) to 7.42×10^{12} cm^{-2}·eV^{-1} (device C). This indicated that the high NH_3 flow in the PECVD process could reduce the surface state and suppress the current collapse.

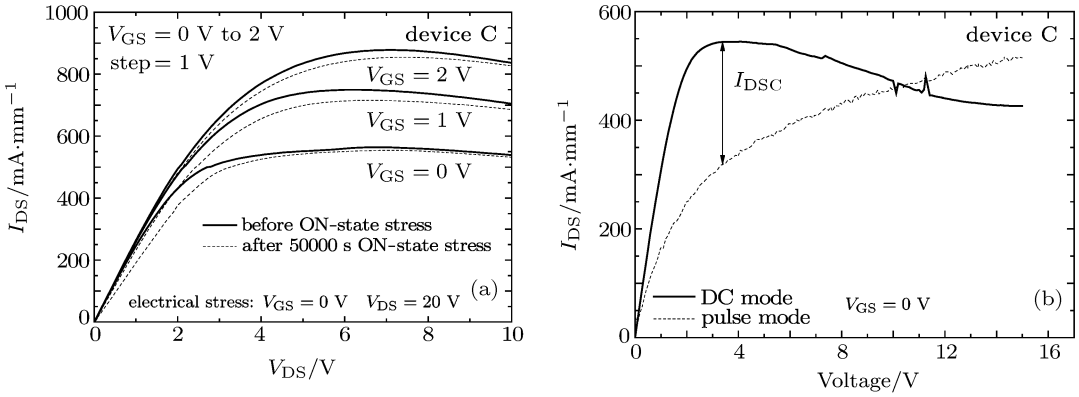


Fig. 9. (a) Source-drain output curves of the 80-nm thickness SiN_x passivated AlGaN/GaN HEMTs (device C). (b) Experimental I_D–V_{DS} characteristics obtained in DC and in the gate turn-on mode.

4. Conclusion

We analysed the electric-field reliability and current collapse of passivated devices, and we found that their influencing factors were different. Under the ON-state stress, the strong electric field leads to electron

trap formation in SiN_x passivation between gate and drain. These electron traps are a main factor for device reliability. Increasing the thickness of passivation can significantly reduce the peak electric-field strength in SiN_x passivation, thereby enhancing the reliability of devices. The high NH_3 flow in the PECVD process is useful for suppressing the current collapse and reducing the surface state. This paper demonstrates that the surface state density has a close relationship with the NH_3 flow in the PECVD process. Only by effectively reducing the density of surface state can we fundamentally suppress the current collapse.

References

[1] Uemoto Y, Shibata D, Yanagihara M, Ishida H, Matsuo H, Nagai S, Batta N, Ming L, Ueda T and Tanaka T 2007 *IEEE IEDM Tech. Digest.* 861

[2] Wu Y F, Kapolnex D and Ibbetson J P 2007 *IEEE IEDM Tech. Digest.* 405

[3] Jimenez J L, Chowdhury U, Kao M Y, Balistreri A, Lee C, Saunier P and Chao P C 2008 *IEEE Int. Rel. Phys. Symp. Proceedings*

[4] Joh J and Alamo J A 2006 *IEEE IEDM Tech. Digest.* 415

[5] Joh J and Alamo J A 2008 *IEEE Electron Dev. Lett.* **29** 287

[6] Zanoni E, Meneghesso G, Verzuesi G and Danesin F 2007 *IEEE IEDM Tech. Digest.* 381

[7] Gu W P, Duan H T, Ni J Y, Hao Y, Zhang J C, Feng Q and Ma X H 2009 *Chin. Phys.* B **18** 1601

[8] Wei W, Lin R B, Hao Y and Feng Q 2008 *Chin. Phys.* B **17** 467

[9] Gu W P, Hao Y, Zhang J C, Wang C, Feng Q and Ma X H 2009 *Acta Phys. Sin.* **58** 511 (in Chinese)

[10] Mittereder J A, Binari S C, Klein P B, Roussos J A, Katzer D S and Storm D F 2003 *Appl. Phys. Lett.* **83** 1650

[11] Sozza A, Dua C, Morvan E, Delage S, Rampazzo F, Tazzoli A, Danesin F and Meneghesso G 2005 *IEEE IEDM Tech. Digest.* 590

[12] Sarua A, Ji H, Kuball M, Uren M J, Martin T, Nash K J, Hilton K P and Balmer R S 2006 *Appl. Phys. Lett.* **88** 103502

[13] Binari S C, Klein P B and Kazior T E 2002 *Proc. IEEE* **9** 1048

[14] Kikkawa T, Nagahara M, Okamoto N, Tateno Y, Yamaguchi Y, Hara N, Joshin K and Asbeck P M 2001 *IEEE IEDM Tech. Digest.* 585

[15] Dieci D, Sozzi G, Menozzi R, Tediosi E, Lanzieri C and Canali C 2001 *IEEE Trans. Electron Devices* **48** 1929

[16] Menozzi R, Cova P, Canali C and Fantini F 1996 *IEEE Trans. Electron Devices* **43** 543

[17] Schroder D K 2006 *Semiconductor Material and Device Characterization* 3rd ed. (Hoboken: Wiley NJ)